in Signal Recovery and Synthesis III, digest of papers, Optical Society of America, pp. 134-137 (invited paper, N. Falmouth, MA, June 1989).

# Phase Error Correction by Shear Averaging

J.R. Fienup

Optical Science Laboratory
Environmental Research Institute of Michigan
P.O. Box 8618, Ann Arbor, MI 48107

## 1. **Introduction**

Synthetic aperture radar (SAR) [1,2] (and other imaging systems) measures the complex Fourier transform (called the signal history or phase history) of the scene being imaged, but it often suffers from one-dimensional (1-D) phase errors due to unknown system platform motion, target motion, system phase instabilities, and propagation through atmospheric turbulence. If uncorrected, these phase errors can cause severe blurring or smearing of the imagery. Phase errors (the residual phase errors remaining after correction for the measured motion) can be corrected by digital phase-error correction (sometimes called autofocus) methods, the most widely used being "sub-aperture processing" and "prominent-point processing." The disadvantage of sub-aperture processing, which is analogous to the concept of a Hartmann sensor in optics, is that it only works for low-order (up to about fourth-order) polynomial-type phase errors. The disadvantage of prominent-point processing, which deconvolves an image based on an estimate of the impulse response of the system, is that it requires the presence of an identifiable, isolated, strong point-like reflector in the scene being imaged. Furthermore, both of these two processing methods require extensive computations.

This paper describes a new phase-error correction method, which we call "shear averaging," that works for arbitrarily high-order, arbitrarily large 1-D phase errors, that requires no prominent points, and is computationally extremely fast. It is based on the *a priori* constraint that the scene being imaged is delta correlated.

## 2. **Historical Perspective**

In a recent publication, Eichel, Ghiglia, and Jakowatz [3] described a phase correction algorithm for SAR. Their key observation was that each range bin of the image is a result of the same fixed phase error (which is a function only of the cross-range or azimuthal coordinate of the signal history) with a different realization of a random process (the complex image in each range bin). Thus it is possible to do some form of averaging in the range dimension, over the random process, in order to get at the fixed quantity, the phase error. They chose to implement this idea using an analogy to the shift-and-add method [4], which would allow them to extract an effective prominent point from the scene even though an identifiable prominent point was not available. However, in astronomy the basic forms of the shift-and-add method, while effective when the image contains a large prominent point, do not work well for diffuse, extended objects.

Other algorithms, such as Knox-Thompson [5] or triple correlation [6], work more reliably and robustly for more general objects. We applied the same idea of averaging in the dimension orthogonal to the dimension of the phase errors, but using an analogy to Knox-Thompson, to develop a much simpler and more elegant algorithm. It can also be viewed as an analogy to wavefront sensing by shearing interferometry, hence the name "shear averaging."

Meanwhile, essentially the same algorithm (but with some differences, as will be explained later) as shear averaging was independently invented by Attia et al., but was only recently published [7]. Attia's algorithm was derived as an extension of the Muller-Buffington method of maximizing image sharpness [8]. Our perspective of the analogy with shearing interferometry (a connection not made by Attia) brings with it additional valuable insights.

3. **Shear Averaging Algorithm**

Let the unaberrated signal history be F(u, v) and the ideal image be its inverse Fourier transform, f(x, y). The aberrated signal history is

$$G(u, v) = F(u, v) \exp[i\phi_e(v)] \, , \tag{1}$$

where $\phi_e(v)$ is the 1-D phase error. In the case of spotlight (polar formatting) SAR [2], u is a frequency coordinate and x is the range coordinate of the image, while v and y are the azimuthal (cross-range) coordinates in signal-history and image spaces, respectively. It is useful to think of v as the pulse (azimuth sample) number. The description that follows will use the language of SAR, although the method applies equally well to other imaging sensors as well.

The shear averaging method consists of the following steps. First, the shear averaged quantity S(v) is formed by computing the average over the sheared product:

$$S(v) = \sum_{u=1}^{N} G(u, v)\, G^*(u, v - a) \, , \tag{2}$$

where N is the number of samples in frequency (or, number of range bins) and a is a fixed number of pulses or azimuth samples. Usually a=1 sample; but, if the signal history is highly oversampled in azimuth, then using a > 1 may be advantageous. Use of multiple values of a would lead to an approach analogous to triple correlation, but here we consider only a single value of a. [In Attia's version of the algorithm, the signal history was already range-compressed, in which case G(u, v) is replaced by G'(x, v), the u-x inverse Fourier transform of G(u, v), and the summation is performed over x, the range bins, which in some cases is equivalent]. The nature of S(v) can be seen by a derivation analagous to that of the van Cittert-Zernike theorem. Inserting Eq. (1) into Eq. (2), approximating the summation over u with an ensemble average (employing an ergodicity argument), and assuming that the object reflectivity is delta-correlated:

$$\langle f(x, y)\, f^*(x - \Delta x, y - \Delta y)\rangle = f_I(x, y)\, \delta(\Delta x, \Delta y) \, , \tag{3}$$

where $f_I(x, y)$ is the underlying incoherent reflectivity of the scene and $\delta$ is a Dirac delta function, one obtains

$$\begin{aligned} S(v) = |S(v)| \exp[i\theta(v)] &\approx N \langle F(u, v)\, F^*(u, v - a)\rangle \exp[i\phi_e(v) - i\phi_e(v - a)] \\ &= N\, \bar{I}\, \mu(0, a) \exp[i\phi_e(v) - i\phi_e(v - a)] \, , \end{aligned} \tag{4}$$

where $\bar{I}$ is the average aperture-plane intensity and $\mu$ is the normalized Fourier transform of $f_I(x, y)$. That is the phase, $\theta(v)$, of S(v) is approximately equal to the difference in phase error from the $(v-a)^{th}$ sample to the $v^{th}$ sample. Therefore, since the constant phase of $\mu(0, a)$ will result only in an inconsequential linear phase term, an estimate of the phase error can be computed according to

$$\hat{\phi}_e(0) = 0 \text{ , and } \quad \hat{\phi}_e(v) = \hat{\phi}_e(v - a) + \theta(v) \tag{5}$$

or

$$\hat{\phi}_e(v) = \sum_{m=1}^{v/a} \theta(ma) \quad . \tag{6}$$

This phase-error estimate is subtracted from the phase of G(u, v) to arrive at a phase-error-corrected version of the signal history:

$$G_{cor}(u, v) = G(u, v) \exp[-i \, \hat{\phi}_e(v)] \quad . \tag{7}$$

Note that addition or subtraction of a phase can be accomplished by a complex phasor multiplication, as shown in Eq. (7).

The analogy of Eq. (2) to shearing interferometry is as follows (the analogy with Knox-Thompson follows similarly). The shearing of the fields is obvious. The G(u, v) are many realizations of the electromagnetic field in the aperture plane (having coordinate v) scattered from the scene, each realization having a different frequency, u. The average over the frequency coordinate, u, is equivalent to averaging over many coherence times. This fact allows us to use results from optical interferometry to predict the variance of $\theta(v)$, the phase difference estimate. Letting N be the number of independent samples summed in the u dimension, and assuming that the "signal-to-noise ratio" $K^2 = |\mu(0, a)|^2 N >> 1$, then from [9, p. 269] the standard deviation of $\theta(v)$ is given by

$$\sigma_\theta = \frac{1}{\sqrt{2}\, K} = \frac{1}{\sqrt{2N}\, |\mu(0, a)|} \quad . \tag{8}$$

If there are M independent samples in azimuth, then the summation of Eq.(6), being over uncorrelated random variables, would have a standard deviation of the phase-error estimate of

$$\sigma_M = \frac{1}{|\mu(0, a)|} \sqrt{\frac{M}{2N}} \quad . \tag{9}$$

Therefore for typical signal histories having M = N and for shear a such that $|\mu(0, a)| \approx 0.7$ (requiring a two-fold oversampling in the v dimension), the expected residual phase error will be about one radian ($\lambda/6$) peak-to-peak, which is small and results in only minor smearing of the imagery.

## 4. **Phase-Error Correction Example**

Figure 1 shows an example of phase-error correction using the shear averaging algorithm for a simulated complex-valued SAR image, consisting of several points with varying phases assigned to the points. Despite the non-randomness of the image (it is not "statistically homogeneous over the area of interest," as demanded by [7]), the phase errors are well corrected.

We have also successfully performed 1-D phase-error correction using the shear averaging algorithm for the case of real, nonnegative objects, which would seem to totally violate the statistical assumptions. Therefore the assumption that the image be delta correlated [Eq. (3)], while sufficient, may not be necessary. The higher spatial-frequency bands for a real, nonnegative object have statistics very similar to those for a diffuse, complex-valued object. That is, a high-pass (or band-pass) filtered image of a real, nonnegative object typically takes on the appearance of a low-pass filtered image of a diffuse, complex-valued object. Correction of 2-D phase errors is also possible by this method, although it is less effective.

## 5. **Conclusion**

Shear averaging has been shown to be a powerful method for correcting 1-D phase errors, based on the (sufficient, but possibly not necessary) constraint that the image be delta correlated. Compared with the Eichel et al. algorithm [3] and with conventional algorithms, it is extremely fast (being non-iterative and not requiring Fourier transforms). The phase-error estimated can be computed for each pulse (azimuth sample) as it comes in, and likewise the correction can be made by Eq. (7) on each pulse as it comes in, without waiting for subsequent pulses. This makes this method easy to implement in real time without requiring large amounts of data buffering. It works over a wide class of objects, even for objects consisting of pure clutter.

This research was supported under ERIM internal research and development funding.

## **References**

1. D.A. Ausherman, A. Kozma, J.L. Walker, H.M. Jones and E.C. Poggio, IEEE Trans. AES-20, 363-400 (1984).
2. J.L. Walker, IEEE Trans. AES-16, 23-52 (1980).
3. P.H. Eichel, D.C. Ghiglia and C.V. Jakowatz, Jr., Opt. Lett. 14, 1-3 (1989).
4. R.H.T. Bates and F.M. Cady, Opt. Commun. 32, 365-369 (1980).
5. K.T. Knox and B.J. Thompson, Astrophys. J. Letters 193, L45-L48 (1974).
6. A.W. Lohmann, G. Weigelt and B. Wirnitzer, Appl Opt. 22, 4028-4037 (1983).
7. E.H. Attia and B.D. Steinberg, IEEE Trans. AP 37, 30-38 (1989).
8. R.A. Muller and A. Buffingtion, J. Opt. Soc. Am. 64, 1200-1210 (1974).
9. J.W. Goodman, Statistical Optics (Wiley, New York, 1985).

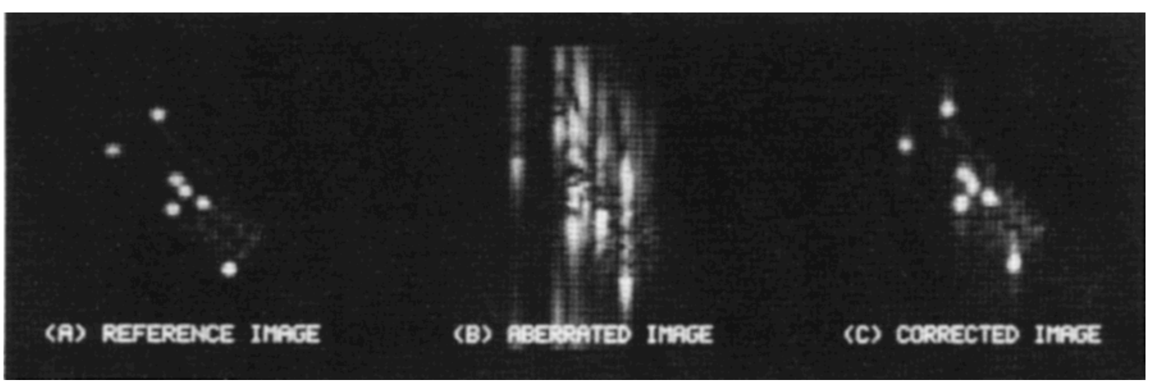


Figure 1. Phase-error correction example. (A) Diffraction-limited image of a synthetic complex-valued object; (B) aberrated image, smeared by 1-D Fourier phase errors in the vertical direction; (C) image obtained from the Fourier transform corrected for phase errors using the shear averaging algorithm.